

## Structure of SrTiO<sub>3</sub> Films on Si

C. Stephen Hellberg\*

*Center for Computational Materials Science, Naval Research Laboratory, Washington, D. C. 20375, USA*

Kristopher E. Andersen<sup>†</sup>

*High Performance Technologies, Inc., Reston, Virginia 20190, USA*

Hao Li<sup>‡</sup>

*Shenzhen New Degree Technology Co., Ltd., Shenzhen, 518054, China*

P. J. Ryan<sup>§</sup>

*Magnetic Materials Group, Argonne National Laboratory, Argonne, Illinois 60439, USA*

J. C. Woicik<sup>||</sup>

*National Institute of Standards and Technology, Gaithersburg, Maryland 20899, USA*

(Received 29 June 2011; revised manuscript received 19 November 2011; published 16 April 2012)

The epitaxial deposition of oxides on silicon opens the possibility of incorporating their diverse properties into silicon-device technology. Deposition of SrTiO<sub>3</sub> on silicon was first reported over a decade ago, but growing the coherent, lattice-matched films that are critical for many applications has been difficult for thicknesses beyond 5 unit cells. Using a combination of density functional calculations and x-ray diffraction measurements, we determine the atomic structure of coherent SrTiO<sub>3</sub> films on silicon, finding that the Sr concentration at the interface varies with the film thickness. The structures with the lowest computed energies best match the x-ray diffraction. During growth, Sr diffuses from the interface to the surface of the film; the increasing difficulty of Sr diffusion with film thickness may cause the disorder seen in thicker films. The identification of this unique thickness-dependent interfacial structure opens the possibility of modifying the interface to improve the thickness and quality of metal oxide films on silicon.

DOI: [10.1103/PhysRevLett.108.166101](https://doi.org/10.1103/PhysRevLett.108.166101)

PACS numbers: 68.55.A-, 61.05.C-, 77.55.Px, 77.80.-e

Oxides exhibit a wide range of functionality ranging from superconductivity to ferroelectricity to ferromagnetism [1,2]. This versatility has driven an enormous research effort over the past decade to combine ordered oxides with semiconductors, especially silicon [3,4]. Growth of SrTiO<sub>3</sub> has received particular emphasis as it is commonly used as a substrate for oxide devices [5,6]. Additionally, the large dielectric constant of SrTiO<sub>3</sub> makes it an attractive gate oxide for electronics, but the conduction band offset of SrTiO<sub>3</sub> on silicon is too small for many device applications [7].

When grown coherently on Si(001), SrTiO<sub>3</sub> is under 1.7% compressive strain, where it is predicted to be ferroelectric in the limit of thick films [8–11]. Ferroelectricity has been observed in thin coherently strained films on silicon, but the films relax beyond about 6 unit cells [12–16].

The atomic structure of the SrTiO<sub>3</sub>/Si interface is as yet unknown; determination of the structure is the goal of this Letter. We find the preferred interface is electrostatically charged and evolves with the thickness of the film. The unusual thickness-dependent structure likely facilitates the relaxation of films seen beyond thicknesses of 5 unit cells.

Numerous structures have been proposed for the interface between SrTiO<sub>3</sub> and Si [6,17–24]. To determine the

correct structure theoretically, we compare the free energies of previously proposed structures and new structures using density functional theory (DFT). In total, we examined 84 different structures using supercells containing as many as  $4 \times 4$  cells [25]. The interface cannot be optimized alone—The surface must be adjusted as well due to its electrostatic coupling with the interface. A key feature of the present approach is that we varied the stoichiometry of both the interface and surface to determine the overall structure minimizing the free energy at each film thickness.

The lowest energy interface is a full SrO layer, shown in Fig. 1(a). As described below, the interface is positively charged. The surface assumes a compensating negative charge by changing its stoichiometry, creating a strong electric field which polarizes the film [10,12]. As growth proceeds, the energy cost of the electric field grows because the volume of the film containing the field grows. To reduce the field, Sr vacancies form at the interface, reducing its charge. The Sr vacancy density at the interface increases continuously with increasing film thickness, shown in Figs. 1(b) and 1(c). At a thickness of 5 unit cells, the predicted structure agrees well with x-ray diffraction measurements of a 5 unit cell film grown coherently on Si(001) [12,26,27].

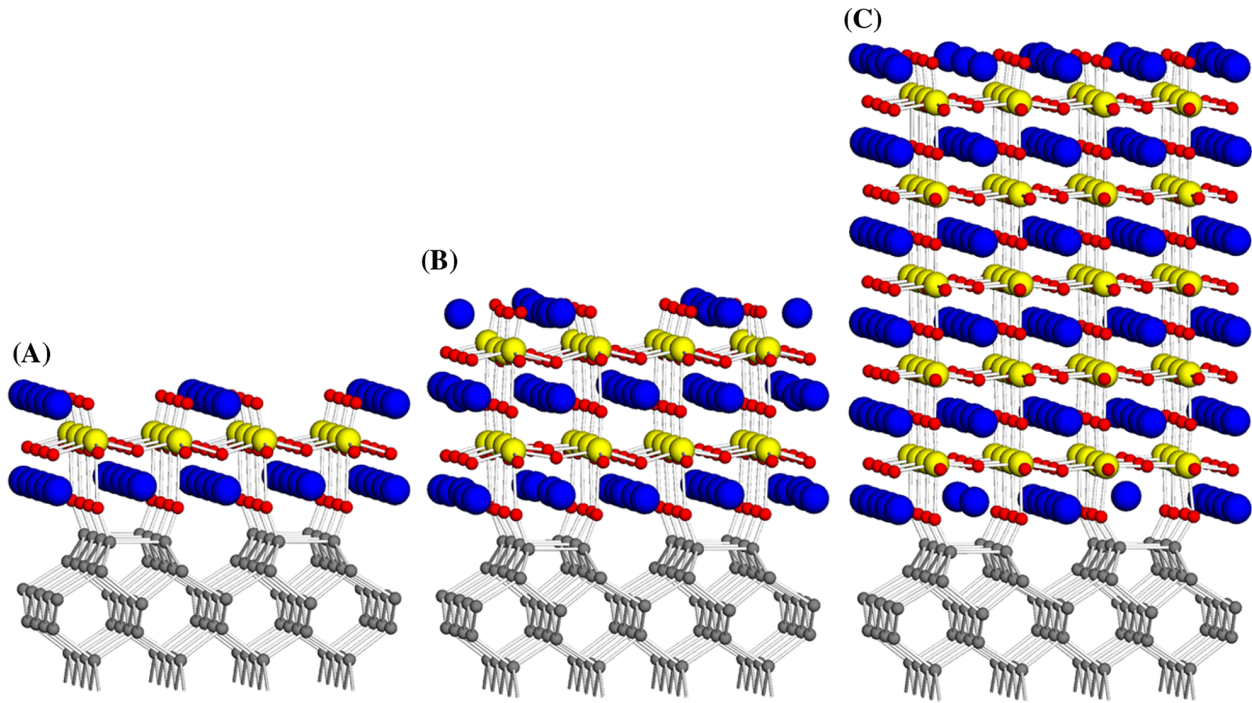


FIG. 1 (color online). The lowest energy structures of  $\text{SrTiO}_3$  films on  $\text{Si}(001)$  at thicknesses of 1 (A), 2 (B), and 5 (C) unit cells. Sr atoms are blue, Ti are yellow, O are red, and Si are grey. The film thicknesses are defined by the number of  $\text{TiO}_2$  layers. The  $\text{SrO}$  interface in (A) is energetically preferred; it is positively charged, and the surface assumes a compensating negative charge by forming Sr vacancies, resulting in a  $\text{Sr}_{1/2}\text{O}$  surface. As the films grow, the charge of the interface is reduced by the formation of Sr vacancies, and the Sr content at the surface increases. At a thickness of 2 unit cells, the optimal interface and surface combination is  $\text{Sr}_{15/16}\text{O}$  (interface) and  $\text{Sr}_{9/16}\text{O}$  (surface), while at 5 unit cells it is  $\text{Sr}_{11/16}\text{O}$  (interface) and  $\text{Sr}_{13/16}\text{O}$  (surface). Note the polarization of the film as indicated by the upward displacement of the Ti atoms. The polarization decreases with increasing film thickness while the rotation of the O octahedra increases.

The lowest energy interface is a full  $\text{SrO}$  layer with oxygens bonded to dimerized surface silicons, shown in Fig. 1(a). The interface is positively charged: Each Sr has nominal charge +2, but each O-Si has charge  $-1$  due to the ionization of the Si by the O [18], yielding a planar charge density of  $+1$  per perovskite cell at the interface. The surface compensates the interfacial charge by forming Sr vacancies. The  $\text{Sr}_{1/2}\text{O}$  surface has a net charge density of  $-1$  per surface cell. The system overall is insulating.

In thicker films, shown in Figs. 1(b) and 1(c), the energy cost of the charged interface is too great, and Sr vacancies form. Writing the interface stoichiometry as  $\text{Sr}_x\text{O}$ , we find  $x$  decreases with increasing thickness. The 2 unit cell film has a  $\text{Sr}_{15/16}\text{O}$  interface, and the 5 unit cell film has a  $\text{Sr}_{11/16}\text{O}$  interface (The calculations use a  $4 \times 4$  supercell [25], which forces  $x$  to be a multiple of  $1/16$ .) The optimal surface, with stoichiometry  $\text{Sr}_y\text{O}$ , always compensates the interfacial charge: In all cases, we find the free energy is minimized when the sum of the charges of the interface and surface is zero, or  $x + y = 3/2$  [28].

The lowest energy modifications to the optimal structure are shifts of Sr ions from the surface to the interface and vice versa which leave  $x + y = 3/2$  invariant [25]. The energy as a function of the interfacial and surface Sr concentration in this low-energy manifold is plotted in

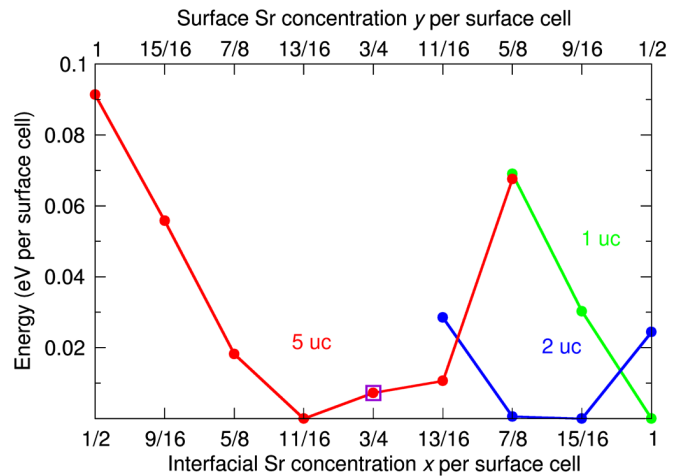


FIG. 2 (color online). Energy as a function of surface and interface Sr concentration for 1, 2, and 5 unit cell films computed with DFT. The stoichiometry of the interface is  $\text{Sr}_x\text{O}$ , the surface is  $\text{Sr}_y\text{O}$ , and  $x + y = 3/2$  is satisfied for these low-energy structures as described in the text. The energies have been shifted so the minimum for each thickness is zero. The structures plotted in Fig. 1 are those with minimal energy for each thickness. The purple square indicates the 5 unit cell structure with a  $\text{Sr}_{3/4}\text{O}$  interface that best agrees with the experimentally measured x-ray diffraction.

Fig. 2 for three film thicknesses. The optimal interfacial Sr concentration decreases with increasing film thickness. By 5 unit cells,  $x = 11/16$  minimizes the energy in DFT, while  $x = 3/4$  agrees best with the x-ray diffraction measurements [25]. We note that scanning transmission electron microscopy images show reduced Sr content at both the interface and surface of the film, supporting this growth model [15,16,24].

The 5 unit cell sample used in the x-ray diffraction measurements was grown coherently on Si(001) by kinetically controlled sequential deposition [12,26]. In order to directly compare the theoretical structures with the experiment, the scattered intensity as a function of scattering vector  $\mathbf{Q}$  for each of the 5 unit cell structures was calculated from

$$I(\mathbf{Q}) = \left| \sum_j f_j(\mathbf{Q}) e^{-i\mathbf{Q} \cdot \mathbf{r}_j} \right|^2, \quad (1)$$

where  $\mathbf{r}_j$  is the atomic position of the  $j$ th theoretical atom and  $f_j$  is its atomic form factor. In each case, the theoretical slabs (i.e., the SrTiO<sub>3</sub> films including the 8 Si underlayers) were added atop a semi-infinite silicon substrate [29]. The theoretical coordinates were rescaled by the ratio of the experimental to theoretical lattice constant of Si. To maintain model independence, no disorder (either thermal vibration or surface roughness) was considered in the calculation of the diffraction patterns, resulting in the more pronounced features in the computed patterns relative to the experiment.

The computed diffraction curves from three low-energy structures [25] are shown with the experimental curve in Fig. 3. Comparing the patterns from the different structures

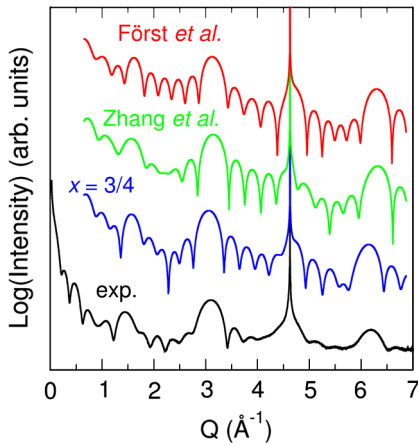


FIG. 3 (color online). The experimental x-ray diffraction curve of a 5 unit cell film of SrTiO<sub>3</sub> on Si(001) compared with calculated curves from three structures with low energies in DFT. The calculated curves use the structures from the Sr<sub>3/2</sub>O<sub>2</sub> interface of Först *et al.*, Ref. [19], the Sr<sub>1/2</sub>O interface of Zhang *et al.*, Ref. [18], and the  $x = 3/4$  structure from the present work. Note the correspondence between the features of the experimental diffraction curves and the  $x = 3/4$  structure that is absent in the other structures.

with the data, it is clear that the features in the  $x = 3/4$  pattern correspond most closely with the features observed by the experiment: (1) the position of the SrTiO<sub>3</sub>(002) diffraction ( $Q = 3.11 \text{ \AA}^{-1}$ ), which is sensitive to the  $c/a$  ratio of the film [12], (2) the structure surrounding the Si(004) diffraction ( $Q = 4.63 \text{ \AA}^{-1}$ ), which is sensitive to the spacing between the bottommost layer of the SrTiO<sub>3</sub> film and the topmost Si layer [29,30], (3) the beating that occurs between the SrTiO<sub>3</sub>(001) ( $Q = 1.45 \text{ \AA}^{-1}$ ) and the SrTiO<sub>3</sub>(002) peaks which is sensitive to the occupation of both the topmost and bottommost SrTiO<sub>3</sub> layers, and (4) the asymmetry of the lobes surrounding the SrTiO<sub>3</sub>(002) diffraction which indicates the polarization of the film [31]. We note that both the asymmetry around the SrTiO<sub>3</sub>(002) diffraction and the enhancement of its Ti K pre-edge feature disappear in thicker relaxed films, thereby confirming their reduced polarization.

The  $c/a$  ratio of the proposed structures is compared directly to the measured ratio in Fig. 4. The  $c/a$  ratio depends sensitively on the polarization of the film. The experimental  $c/a$  ratios from 5 and 10 unit cell films are significantly greater than those predicted from the elastic constants of SrTiO<sub>3</sub> [32] and agree well with calculations on bulk strained SrTiO<sub>3</sub>, which show it is polarized [8,10]. Of the low-energy structures in DFT, the  $x = 3/4$  structure agrees best with the experimental  $c/a$ .

Both SrTiO<sub>3</sub> and silicon are “nonpolar” materials in the (001) direction—each atomic layer is nominally charge neutral. Nevertheless, we find that the favored interface between SrTiO<sub>3</sub> and silicon is *positively* charged. A

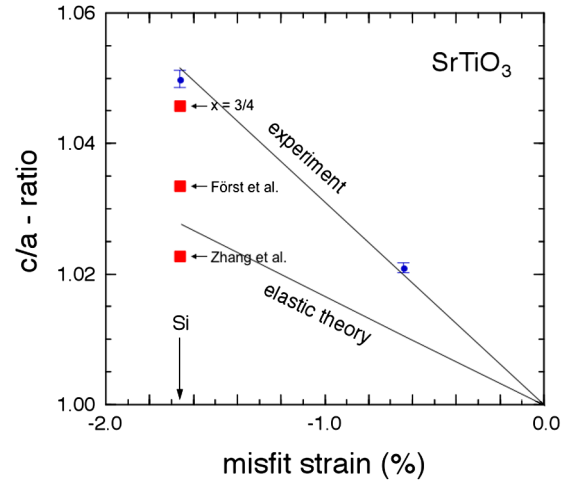


FIG. 4 (color online). The  $c/a$  ratio as a function of in-plane strain. Measured values for 5 and 10 unit cell SrTiO<sub>3</sub> films on Si(001), determined from the SrTiO<sub>3</sub>(002) and (202) diffraction peaks, are plotted in blue with error bars [12,36]. The 5 unit cell film is under approximately  $-1.7\%$  strain and is coherent with the Si substrate. The 10 unit cell film has substantially relaxed. The red squares show  $c/a$  ratios computed from three theoretical 5 unit cell structures with low free energies: the  $x = 3/4$  structure, the Sr<sub>3/2</sub>O<sub>2</sub> interface of Först *et al.*, Ref. [19], and the Sr<sub>1/2</sub>O interface of Zhang *et al.*, Ref. [18].

compensating *negative* charge forms on the surface of the SrTiO<sub>3</sub> film, and the resulting field between interface and surface strongly polarizes the film [12,22–24]. The energy cost of this field grows with film thickness, and the optimal charge of the interface and surface is reduced with increasing film thickness. The reduction of charge is achieved by the formation of Sr vacancies at the interface and migration of Sr ions to the surface.

A related system, LaAlO<sub>3</sub> films on SrTiO<sub>3</sub>, also forms a charged interface that is compensated by the surface [33–35]. Here the charge originates from the growth of “polar” LaAlO<sub>3</sub> on “nonpolar” SrTiO<sub>3</sub>. Just as in the case of SrTiO<sub>3</sub>/Si, the electrostatic energy diverges as the film grows thicker, and the system must reconstruct. Instead of moving cations from the interface to the surface as occurs in SrTiO<sub>3</sub>/Si, electrons move from the LaAlO<sub>3</sub> surface to the interface, reducing its charge and forming an electron gas.

We believe the movement of Sr ions may provide the electrostatic compensation for the switchable polarization recently observed in such films [16]. Additionally, the migration of Sr ions during growth could facilitate the relaxation of films at thicknesses beyond 5–6 unit cells. The determination of the atomic structure of the growing films presented here may lead to engineered surface modifications (for example by doping) which avoid the charged interface, potentially shifting the band offsets and improving the quality and thickness of the films.

We thank Christopher R. Ashman, Noam Bernstein, and Steven C. Erwin for useful discussions. The film deposition was conducted at the former Motorola Labs in Tempe, Arizona. The Advanced Photon Source is supported by the U.S. Department of Energy, Basic Energy Sciences, Office of Science under Contract No. W-31-109-ENG-38. Computations were performed at the AFRL and ERDC DoD Major Shared Resource Centers.

\*hellberg@nrl.navy.mil

†kreander@ccs.nrl.navy.mil

‡h.li@newdegreetech.com

§pryan@aps.anl.gov

||woicik@bnl.gov

- [1] J. W. Reiner, A. M. Kolpak, Y. Segal, K. F. Garrity, S. Ismail-Beigi, C. H. Ahn, and F. J. Walker, *Adv. Mater.* **22**, 2919 (2010).
- [2] J. W. Park, D. F. Bogorin, C. Cen, D. A. Felker, Y. Zhang, C. T. Nelson, C. W. Bark, C. M. Folkman, X. Q. Pan, M. S. Rzechowski *et al.*, *Nature Commun.* **1**, 94 (2010).
- [3] J. Robertson, *Rep. Prog. Phys.* **69**, 327 (2006).
- [4] D. G. Schlom, L.-Q. Chen, X. Pan, A. Schmehl, and M. A. Zurbuchen, *J. Am. Ceram. Soc.* **91**, 2429 (2008).
- [5] H. Mori and H. Ishiwara, *Jpn. J. Appl. Phys., Part 2* **30**, L1415 (1991).
- [6] R. A. McKee, F. J. Walker, and M. F. Chisholm, *Phys. Rev. Lett.* **81**, 3014 (1998).
- [7] S. A. Chambers, Y. Liang, Z. Yu, R. Droopad, J. Ramdani, and K. Eisenbeiser, *Appl. Phys. Lett.* **77**, 1662 (2000).
- [8] N. A. Pertsev, A. K. Tagantsev, and N. Setter, *Phys. Rev. B* **61**, R825 (2000).
- [9] J. Levy, *Phys. Rev. A* **64**, 052306 (2001).
- [10] A. Antons, J. B. Neaton, K. M. Rabe, and D. Vanderbilt, *Phys. Rev. B* **71**, 024102 (2005).
- [11] C. R. Ashman, C. S. Hellberg, and S. Halilov, *Phys. Rev. B* **82**, 024112 (2010).
- [12] J. C. Woicik, H. Li, P. Zschack, E. Karapetrova, P. Ryan, C. R. Ashman, and C. S. Hellberg, *Phys. Rev. B* **73**, 024112 (2006).
- [13] J. C. Woicik, E. L. Shirley, C. S. Hellberg, K. E. Andersen, S. Sambasivan, D. A. Fischer, B. D. Chapman, E. A. Stern, P. Ryan, D. L. Ederer *et al.*, *Phys. Rev. B* **75**, 140103 (2007).
- [14] L. F. Kourkoutis, C. S. Hellberg, V. Vaithyanathan, H. Li, M. K. Parker, K. E. Andersen, D. G. Schlom, and D. A. Muller, *Phys. Rev. Lett.* **100**, 036101 (2008).
- [15] S.-B. Mi, C.-L. Jia, V. Vaithyanathan, L. Houben, J. Schubert, D. G. Schlom, and K. Urban, *Appl. Phys. Lett.* **93**, 101913 (2008).
- [16] M. P. Warusawithana, C. Cen, C. R. Sleasman, J. C. Woicik, Y. Li, L. F. Kourkoutis, J. A. Klug, H. Li, P. Ryan, L.-P. Wang *et al.*, *Science* **324**, 367 (2009).
- [17] P. W. Peacock and J. Robertson, *Appl. Phys. Lett.* **83**, 5497 (2003).
- [18] X. Zhang, A. A. Demkov, H. Li, X. Hu, Y. Wei, and J. Kulik, *Phys. Rev. B* **68**, 125323 (2003).
- [19] C. J. Först, C. R. Ashman, K. Schwarz, and P. E. Blöchl, *Nature (London)* **427**, 53 (2004).
- [20] I. N. Yakovkin and M. Gutowski, *Phys. Rev. B* **70**, 165319 (2004).
- [21] X. F. Wang, J. Wang, Q. Li, M. S. Moreno, X. Y. Zhou, J. Y. Dai, Y. Wang, and D. Tang, *J. Phys. D* **42**, 085409 (2009).
- [22] A. M. Kolpak, F. J. Walker, J. W. Reiner, Y. Segal, D. Su, M. S. Sawicki, C. C. Broadbridge, Z. Zhang, Y. Zhu, C. H. Ahn *et al.*, *Phys. Rev. Lett.* **105**, 217601 (2010).
- [23] A. M. Kolpak and S. Ismail-Beigi, *Phys. Rev. B* **83**, 165318 (2011).
- [24] D. P. Kumah, J. W. Reiner, Y. Segal, A. M. Kolpak, Z. Zhang, D. Su, Y. Zhu, M. S. Sawicki, C. C. Broadbridge, C. H. Ahn *et al.*, *Appl. Phys. Lett.* **97**, 251902 (2010).
- [25] See Supplemental Material at <http://link.aps.org/supplemental/10.1103/PhysRevLett.108.166101> for details on the computations and the experiments.
- [26] H. Li, X. Hu, Y. Wei, Z. Yu, X. Zhang, R. Droopad, A. A. Demkov, J. J. Edwards, K. Moore, W. Ooms *et al.*, *J. Appl. Phys.* **93**, 4521 (2003).
- [27] F. S. Aguirre-Tostado, A. Herrera-Gómez, J. C. Woicik, R. Droopad, Z. Yu, D. G. Schlom, P. Zschack, E. Karapetrova, P. Pianetta, and C. S. Hellberg, *Phys. Rev. B* **70**, 201403 (2004).
- [28] The Sr<sub>y</sub>O surface has nominal charge  $\sigma_{\text{surf}} = 2y - 2$ ; the Sr<sub>x</sub>O interface has nominal charge  $\sigma_{\text{int}} = 2x - 1$  due to the ionization of the Si. Charge neutrality,  $\sigma_{\text{int}} + \sigma_{\text{surf}} = 0$ , yields  $x + y = 3/2$ .
- [29] I. K. Robinson, R. T. Tung, and R. Feidenhans'l, *Phys. Rev. B* **38**, 3632 (1988).

- [30] Y. Segal, J. W. Reiner, A. M. Kolpak, Z. Zhang, S. Ismail-Beigi, C. H. Ahn, and F. J. Walker, *Phys. Rev. Lett.* **102**, 116101 (2009).
- [31] C. Thompson, C. Foster, J. Eastman, and G. Stephenson, *Appl. Phys. Lett.* **71**, 3516 (1997).
- [32] R. O. Bell and G. Rupprecht, *Phys. Rev.* **129**, 90 (1963).
- [33] A. Ohtomo, D. A. Muller, J. L. Grazul, and H. Y. Hwang, *Nature (London)* **419**, 378 (2002).
- [34] N. Nakagawa, H. Y. Hwang, and D. A. Muller, *Nature Mater.* **5**, 204 (2006).
- [35] C. Cen, S. Thiel, G. Hammerl, C. W. Schneider, K. E. Andersen, C. S. Hellberg, J. Mannhart, and J. Levy, *Nature Mater.* **7**, 298 (2008).
- [36] P. Ryan, D. Wermeille, J. W. Kim, J. C. Woicik, C. S. Hellberg, and H. Li, *Appl. Phys. Lett.* **90**, 221908 (2007).